Cancer Cell
Article

Hematopoietic Stem Cell Expansion Precedes the Generation of Committed Myeloid Leukemia-Initiating Cells in C/EBPα Mutant AML

Oxana Bereshchenko,[1] Elena Mancini,[1] Susan Moore,[1] Daniel Bilbao,[1] Robert Månsson,[2] Sidinh Luc,[3] Amit Grover,[1] Sten Eirik W. Jacobsen,[3] David Bryder,[2] and Claus Nerlov[1,4,*]
[1]EMBL Mouse Biology Unit, Via Ramarini 32, 00015 Monterotondo, Italy
[2]Hematopoietic Stem Cell Laboratory, University of Lund, 221 84 Lund, Sweden
[3]Haemopoietic Stem Cell Laboratory, Weatherall Institute for Molecular Medicine, University of Oxford, Oxford, UK
[4]Institute for Stem Cell Research, University of Edinburgh, Edinburgh, UK
*Correspondence: cnerlov@staffmail.ed.ac.uk
DOI 10.1016/j.ccr.2009.09.036

SUMMARY

We here use knockin mutagenesis in the mouse to model the spectrum of acquired *CEBPA* mutations in human acute myeloid leukemia. We find that C-terminal C/EBPα mutations increase the proliferation of long-term hematopoietic stem cells (LT-HSCs) in a cell-intrinsic manner and override normal HSC homeostasis, leading to expansion of premalignant HSCs. However, such mutations impair myeloid programming of HSCs and block myeloid lineage commitment when homozygous. In contrast, N-terminal C/EBPα mutations are silent with regards to HSC expansion, but allow the formation of committed myeloid progenitors, the templates for leukemia-initiating cells. The combination of N- and C-terminal C/EBPα mutations incorporates both features, accelerating disease development and explaining the clinical prevalence of this configuration of *CEBPA* mutations.

INTRODUCTION

A large body of evidence indicates that acute myeloid leukemia (AML) arises through the stepwise acquisition of genetic and epigenetic changes. In particular, tumorigenesis is promoted by the collaboration between mutations affecting signaling pathways (class I or signaling mutations; *FLT3*, *RAS* and *KIT* mutations) and mutations with a transcriptional/nuclear function (class II or initiating mutations, balanced translocations, and *CEBPA* and *NPM1* mutations) (Kelly and Gilliland, 2002; Moore, 2005). Because the hematopoietic stem cell (HSC) is the only long-lived cell within the myeloid differentiation hierarchy, it is the primary candidate cell for the accumulation of these successive leukemogenic events. Studies of AML patients relapsing from complete remission after chemotherapy are consistent with class II (or initiating) mutations, including balanced translocations and *CEBPA* mutations, being very early events in this process, because these events are generally conserved in the relapse tumor (Shih et al., 2006). In contrast, *KIT*, *FLT3,* and *RAS* mutations (class I or signaling mutations) frequently differ between initial and relapse tumors (Kottaridis et al., 2002; Shih et al., 2002, 2004), indicating that they occur subsequently to the highly conserved class II mutations. However, despite the inferred founding nature of class II mutations, limited information exists about their effect on HSCs, and in particular their ability to cause expansion of premalignant stem cell populations, thereby increasing the probability of acquisition of collaborating genetic/epigenetic events.

This issue has been highlighted by the recent controversy regarding the role of the HSC compartment in AML maintenance. The original observations by Dick and colleagues identified the leukemia-initiating cell (LIC) as $CD34^{+}CD38^{-}$ (Bonnet and Dick, 1997; Lapidot et al., 1994), consistent with an immature

SIGNIFICANCE

Acquired mutations in the *CEBPA* gene occur in ca. 9% of human AML patients. However, so far no explanation existed for the observation that ca. 90% of patients have distinct mutations on the two *CEBPA* alleles. Our findings provide a cellular basis for the observed clinical mutation pattern. Significantly, the leukemia-initiating cells that develop in mice with HSC expansion are committed progenitors, suggesting that leukemogenic mutations may have crucial functions in cell types not found in the final transformed clone. Finally, we demonstrate that impaired myeloid lineage commitment of *Cebpa* mutant HSCs is preceded by a loss of myeloid gene expression at the HSC level, providing a link between myeloid programming of HSCs and their lineage potential.

HSC-like phenotype. Here mutations that increase HSC proliferation and/or self-renewal would provide a selective advantage to premalignant HSCs, and in cooperation with second hits lead to transformation. However, recent results indicate that the lack of detectable LIC activity in the $CD34^+CD38^+$ progenitor fraction was due primarily to Fc-mediated immune clearance of anti-CD38 conjugated cells. If this is circumvented, LICs with a myeloid progenitor phenotype ($CD34^+CD38^+$) are more abundant in the majority of AML cases studied (Taussig et al., 2008). In such a scenario, premalignant HSC expansion, lineage commitment, and target cell transformation could become rate-limiting features of initiating mutations, requiring the effects of oncogenic mutations on several aspects of hematopoiesis to be examined. For proper assessment of these effects, the disease models need to model the human disease as accurately as possible. As an example, viral expression of MLL-AF9 allows leukemia initiation from a committed granulocyte-macrophage progenitor (GMP) (Cozzio et al., 2003), whereas a knockin *Mll-Af9* allele, driven by the endogenous *Mll1* promoter, could initiate AML only from HSCs (Chen et al., 2008), presumably because of the low activity of the *Mll1* promoter in myeloid progenitors.

This consideration is particularly relevant in the case of *CEBPA* mutations because deletion of the *Cebpa* gene from murine HSCs was found to make HSCs more competitive against wild-type HSCs (Zhang et al., 2004). Although this would be consistent with *CEBPA* mutations having a similar function in preleukemic HSCs, such an interpretation is complicated by the finding that leukemia-derived *CEBPA* mutations are virtually never null mutations. Rather, *CEBPA* mutations are divided into two major groups: N-terminal mutations that block the translation of the 42 kDa isoform (p42) while allowing the 30 kDa isoform (p30) to be expressed and C-terminal mutations that generate in-frame insertions/deletions within the basic region-leucine zipper DNA binding domain (Leroy et al., 2005; Nerlov, 2004). Notably, >90% of leukemias with bialleleic *CEBPA* mutations harbor one allele with a C-terminal mutation and one with an N-terminal mutation, indicating selection of this mutation pattern during tumorigenesis. In contrast, tumors with homozygous N- or C-terminal mutations are comparatively rare (Pabst and Mueller, 2007). This indicates that the two mutations provide distinct leukemogenic functions and thus are able to collaborate. The importance of specific alterations of C/EBPα function is further supported by the finding that complete deletion of *Cebpa* does not lead to leukemia in the mouse (Heath et al., 2004; Zhang et al., 2004). C/EBPα is generally considered an inducer of terminal differentiation due to its ability to couple induction of cell-type-specific gene expression to cell-cycle arrest (Nerlov, 2007), and in the mouse *Cebpa* mutations that impair E2F repression by C/EBPα increase myeloid progenitor proliferation (Kirstetter et al., 2008; Porse et al., 2005) and impair terminal granulopoiesis (Porse et al., 2001). Complete deletion of *Cebpa* blocks the formation of GMPs and thus myeloid lineage commitment (Zhang et al., 2004). However, despite the relevance of C/EBPα to HSC function, little is known about its role in HSC gene expression, and how this may impact proliferation, lineage commitment, and leukemogenesis. In particular, the complex nature of AML-derived *CEBPA* mutations indicates a need to understand the specific impact of patient-derived mutant alleles on HSC homeostasis and the myeloid differentiation pathway.

RESULTS

To resolve this question, we decided to generate an accurate mouse model for the spectrum of *CEBPA* mutations occurring in AML (Figure 1A). We generated a knockin allele mimicking one of the common C-terminal mutations (K313 duplication: K313KK or K allele; Figure 1B). By combining this mutation with an existing knockin of an N-terminal mutation (Lp30 or L allele [Kirstetter et al., 2008]) (Figure 1B), the spectrum of patient mutations could be generated. Fetal liver (FL) cells from K/K, K/L, L/L, and +/+ mice (CD45.2 allotype) were competitively transplanted into lethally irradiated CD45.1/2 recipients along with CD45.1 wild-type competitor bone marrow cells (Figure 1C). In this manner, lethality due to dysfunction of *Cebpa* mutant cells was avoided, and mutant HSC behavior could be studied while competing with wild-type HSCs, a situation more similar to that encountered in the premalignant state. Importantly, the frequency of phenotypic HSCs in the FL, measured either as Lin^- $Sca\text{-}1^+$ $c\text{-}Kit^+$ cells (LSK cells; data not shown) or LSK $AA4.1^+$ cells (repopulating HSC fraction (Jordan et al., 1995); Figure 1D), did not differ between the mutant genotypes.

Analysis of mice 4.5 weeks after competitive transplantation revealed that the frequency of LSK cells was increased relative to +/+ controls in K/L and K/K (but not L/L) mice, indicating loss of HSC homeostasis (Figure 2A). This increase was due to specific expansion of the mutant HSC pool (Figure 2B), demonstrating a cell-intrinsic effect of these *Cebpa* mutations. Fractionation of the experimental ($CD45.2^+CD45.1^-$) HSC compartment using CD150 and Flt3 expression (Figure 2C) showed expansion of all phenotypic HSC subsets, most significantly the short-term (ST)-HSC ($CD150^-Flt3^-$) and lymphoid-primed multipotent progenitor (LMPP) ($CD150^-Flt3^+$) populations, although mild expansion was observed also of long-term (LT)-HSCs ($CD150^+$ $Flt3^-$) (Figure 2D). Interestingly, K/+ HSCs did not expand in this setting (see Figure S1 available online), suggesting that mutation of both *Cebpa* alleles is required for the effect of C-terminal C/EBPα mutation on HSC expansion to take effect. Importantly, *Cebpa* mRNA was expressed in all three HSC fractions (Figure 2E), consistent with the effects of *Cebpa* mutation being cell intrinsic.

To probe the molecular basis for the observed HSC expansion, we performed Affymetrix-based global gene expression analysis on sorted $CD45.2^+CD45.1^-$ LSK cells from competitively transplanted animals. LIMMA analysis of differentially expressed genes (Table S1) followed by unsupervised clustering showed that the nonhomeostatic K/L and K/K LSK populations coclustered, as did the L/L and +/+ LSK cells (Figure 3A). Gene expression signatures of expanding HSC populations have been generated by microarray analysis of the quiescence-proliferation-quiescence sequence induced by 5-fluorouracil treatment (Venezia et al., 2004). Using gene set enrichment analysis (GSEA), we observed that the expression of quiescence-associated genes (Q-Sig) was significantly decreased in expanding (K/K and K/L) relative to homeostatic (L/L and +/+) LSK cells, whereas no significant enrichment of proliferation-associated gene expression was observed (Figure 3B). Comparison of individual mutant LSK populations to +/+ LSK cells showed that K/K and K/L LSK cells, but not L/L LSK cells, were depleted of Q-Sig genes (Figure 3C). Because the LT-HSC population gives rise to

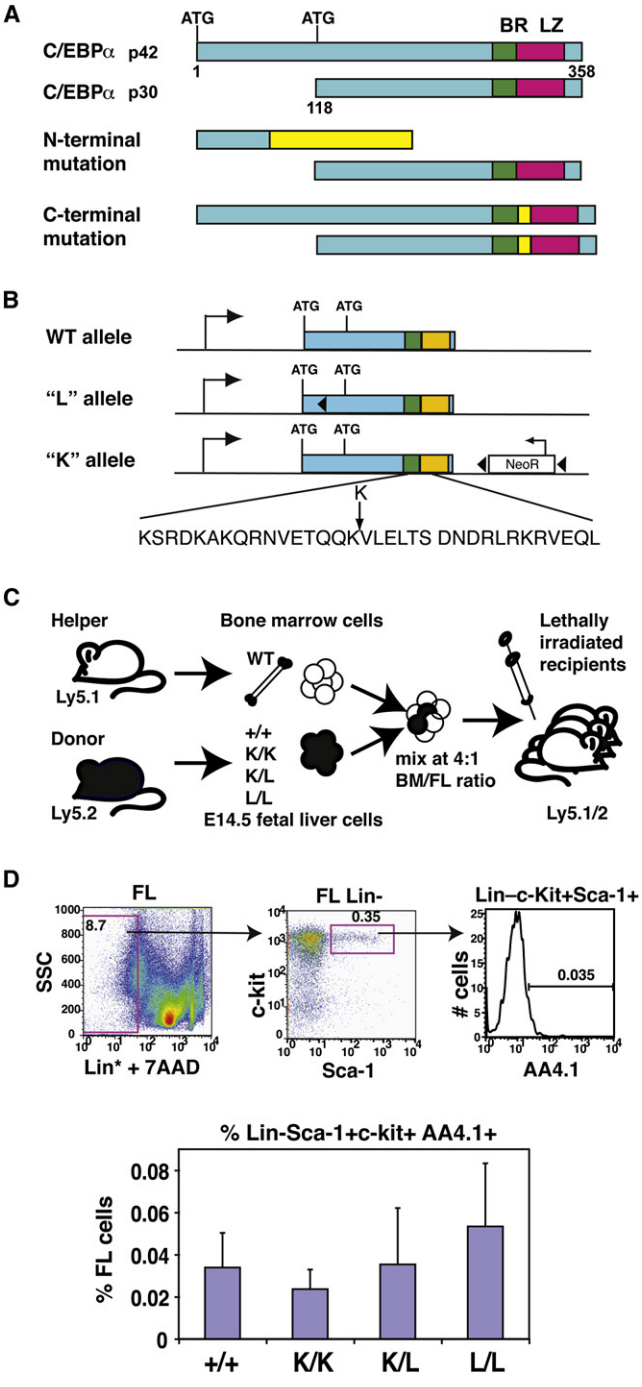

Figure 1. Modeling *Cebpa* Mutant AML In Vivo

(A) Schematic representation of C/EBPα protein isoforms occurring naturally (p42 and p30) and as a result of AML associated mutations. BR, basic region; LZ, leucine zipper.

(B) Schematic representation of mutant *Cebpa* alleles. Closed triangles, LoxP sites; open box, neomycin cassette; duplicated lysine residue is shown in red.

(C) Experimental design for generation of radiation chimeras to study the effect of compound *Cebpa* mutations on hematopoiesis. A total of 1.25×10^5 fetal liver (FL) cells (Ly5.2 allotype and indicated genotypes) were tail vain injected into lethally irradiated recipients (CD45.1/2 allotype) along with 5×10^5 wild type helper bone marrow (BM) cells (CD45.1 allotype).

(D) Evaluation of frequencies of hematopoietic stem cell in E14.5 FLs of *Cebpa* allelic variants and their combination. Live, Lin^- cells were gated and analyzed for the expression of the c Kit and Sca 1 surface markers. Lin^-c $Kit^+Sca\ 1^+$ (LSK) cells were gated and further analyzed for the expression of AA4.1 surface marker. The gating strategy and representative fluorescence activated cell sorting (FACS) plots are shown for *Cebpa* wild type (WT) FL. The percentages of each population relative to whole FL are shown next to each gate. Graphs below the plots represent average of LSK and LSK $AA4.1^+$ frequencies (five independent experiments, total of three to nine FLs per genotype). Error bars represent the standard deviation.

the other LSK subsets, any defect in proliferation control could originate in this cell population. Similar gene profiling of K/L against +/+ control LT-HSCs (Table S2) showed that Q-Sig genes were also depleted in *Cebpa* mutant cells (Figure 3D).

To address whether depletion of the quiescence signature was associated with increased proliferation, we performed flow cytometry-based cell-cycle analysis. Through intracellular staining for Ki67 and DNA content (using DAPI), we could define G0 HSCs ($Ki67-$, 2n DNA content), G1 ($Ki67^+$, 2n), and S/G2/M ($Ki67^+$, > 2n) populations within the HSC subfractions (Figure 3E). The K/L and K/K mutant HSCs showed a decreased G0 fraction, and correspondingly increased G1 and/or S/G2M fractions in LT-HSCs (Figure 3F). Similar results were obtained for the other HSC subsets (Figures 3G and 3H), whereas L/L HSCs did not differ significantly from +/+ controls. We were therefore able to conclude that introduction of the K/K or K/L mutations into the HSC compartment caused expansion of the mutant HSC/multipotent progenitor (MPP) containing LSK population through a cell-intrinsic mechanism, mediated in part by decreased quiescence of *Cebpa* mutant phenotypic LT-HSCs and their downstream progeny. This expansion did not continue in the progenitor compartment because the $Lin^-Sca\text{-}1^-c\text{-}Kit^+$ populations were proportional to the LSK populations (data not shown), indicating the HSC compartment as the important point of expansion.

Expansion of a premalignant HSC/MPP compartment is a potentially potent accelerator of leukemogenesis because it increases the pool of transformable stem cells and/or progenitors. To compare the leukemogenic potential of the different combinations of *Cebpa* mutations, we monitored cohorts of K/K, L/L, K/L, and control +/+ fetal liver transplanted chimeras for survival and tumor development. All three mutant genotypes gave rise to lethal leukemias. However, we observed that mice transplanted with K/L FL cells died significantly more quickly than the L/L and K/K cohorts (Figure 4A), whereas the K/K disease development was delayed compared to the other mutations. We had previously characterized the LIC in L/L homozygous mice as a committed myeloid progenitor ($Sca\text{-}1^-Mac\text{-}1^{lo/+}c\text{-}Kit^+$ [Kirstetter et al., 2008]). To determine whether the accelerated disease induced by the K/L mutation was due to the transformation of a different target cell, we performed fractionation of the leukemias into an HSC-containing fraction ($Sca\text{-}1^+$; fraction I), a myeloid progenitor fraction ($Sca\text{-}1^-Mac\text{-}1^{lo/+}c\text{-}Kit^+$; fraction II), and a differentiated tumor cell fraction ($Sca\text{-}1^-Mac\text{-}1^{hi}c\text{-}Kit^{lo/-}$; fraction III) (Figure 4B). Upon transplantation into lethally irradiated recipients (CD45.1/2) along with CD45.1 competitor, only fraction II gave rise to lethal leukemia (Figure 4C) associated with unilineage myeloid engraftment (Figure 4D). Interestingly, in two of three leukemic mice, the HSC-containing fraction I yielded long-term multilineage engraftment

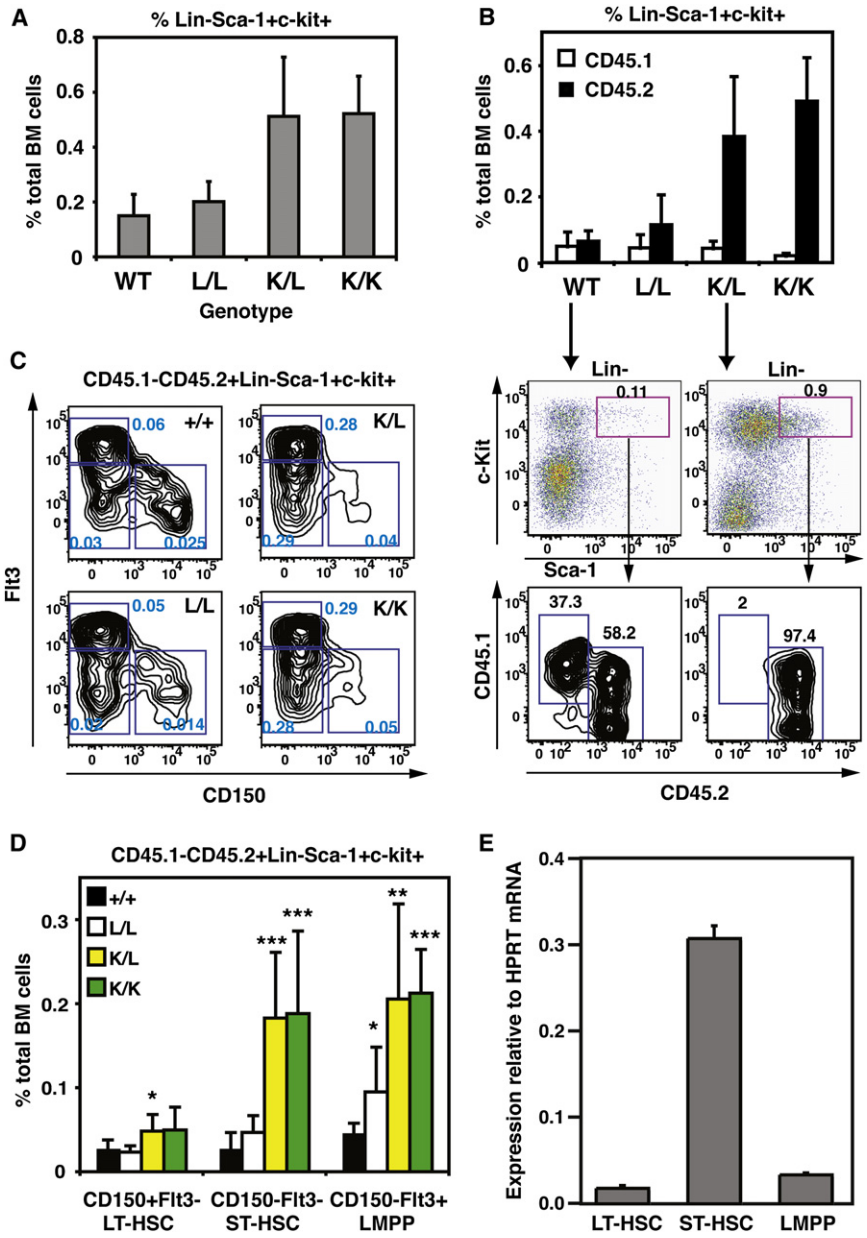

Figure 2. Expansion of C/EBPα Mutant HSCs

(A) Frequency of LSK cells in BM of mice competitively transplanted with wild type or *Cebpa* mutant FL (genotypes indicated) along with wild type BM helper cells. Graphs represent average of three independent experiments, each with three mice per genotype.

(B) LSK compartment was analyzed for the relative contribution of FL derived (CD45.2$^+$, black bars) and helper BM derived cells (CD45.1$^+$, white bars). Representative dot plots for the LSK gates and allotype based fractionation of LSK compartment are shown below the graph for WT and K/L FL cell transplanted animals.

(C) LSK CD45.2$^+$ compartment was subfractioned into LT HSC, ST HSC, and MPP based on the surface expression of CD150 and Flt3.

(D) Graphs represent frequencies of LSK subpopulations within CD45.2$^+$ FL derived cells of the four indicated genotypes (color coded). Data represent average of two independent experiments, three mice per genotype with standard deviation and statistical significance shown (*$p < 0.05$; **$p < 0.005$; ***$p < 0.0005$, t test; error bars indicate standard deviations). Representative contour plots of Flt3 and CD150 expression based fractionation of CD45.1$^-$CD45.2$^+$ LSK cells are shown below the graph for each of the genotypes. Numbers within each window represent frequency of each subpopulation of total bone marrow cells.

(E) Expression of *Cebpa* mRNA was measured by TaqMan RT PCR in the LT HSC, ST HSC, and LMPP fractions. Values represent the average of three independent sorting experiments, each measured in triplicate. Values were normalized to those obtained in the same samples for *Hprt* mRNA. In all panels, error bars represent standard deviations.

with no leukemia observed within 4 months (Figures 4C and 4D and data not shown). The more rapid K/L leukemia is thus driven by a committed myeloid progenitor with leukemia-initiating activity in the HSC fraction below the limit of detection at the cell dosage used. Importantly, direct transplantation of sorted myeloid progenitors (Lin$^-$Sca-1$^-$c-Kit$^+$) from K/L FL did not result in any engraftment, which was observed only when transplanting the LSK fraction (data not shown).

These results were consistent with preleukemic HSC expansion accelerating K/L leukemogenesis by generating high numbers of committed progenitor templates for transformation. However, the slow progression of the K/K leukemias could not be explained in this manner. A closer examination of the end-stage disease revealed that K/L and L/L tumors were virtually always granulocytic. They contained myeloid blasts in the peripheral blood (Figure 5A) and showed partial granulocytic maturation of tumor cells (Figure 5B), with myeloid infiltrates of the spleen (Figure 5C) that stained positive for myeloperoxidase (Figure 5D), consistent with an FAB M2-like leukemia (granulocytic with maturation). However, only ~25% of K/K tumors could be classified as myeloid with maturation based on the above criteria (Figures 5A–5E; K/K-M phenotype), with the remaining tumors displaying a more immature phenotype (K/K-I phenotype) with undetectable maturation or myeloid infiltration. Flow cytometry of the mutant bone marrow fraction (Figure 5F) confirmed that the K/K-I phenotype contained very few differentiating myeloid cells (Mac-1^{hi}c-Kit$^{-/lo}$). Rather, the K/K-I mice were characterized by the accumulation of immature erythroid cells, indicating leukemia with erythroid lineage involvement (data not shown). These results are summarized in Figure 5G.

This suggested that K/K mutant cells were impaired in the generation of myeloid tumors with granulocytic maturation, such as those sustained by the previously characterized committed myeloid LIC. We have previously found that C/EBPα

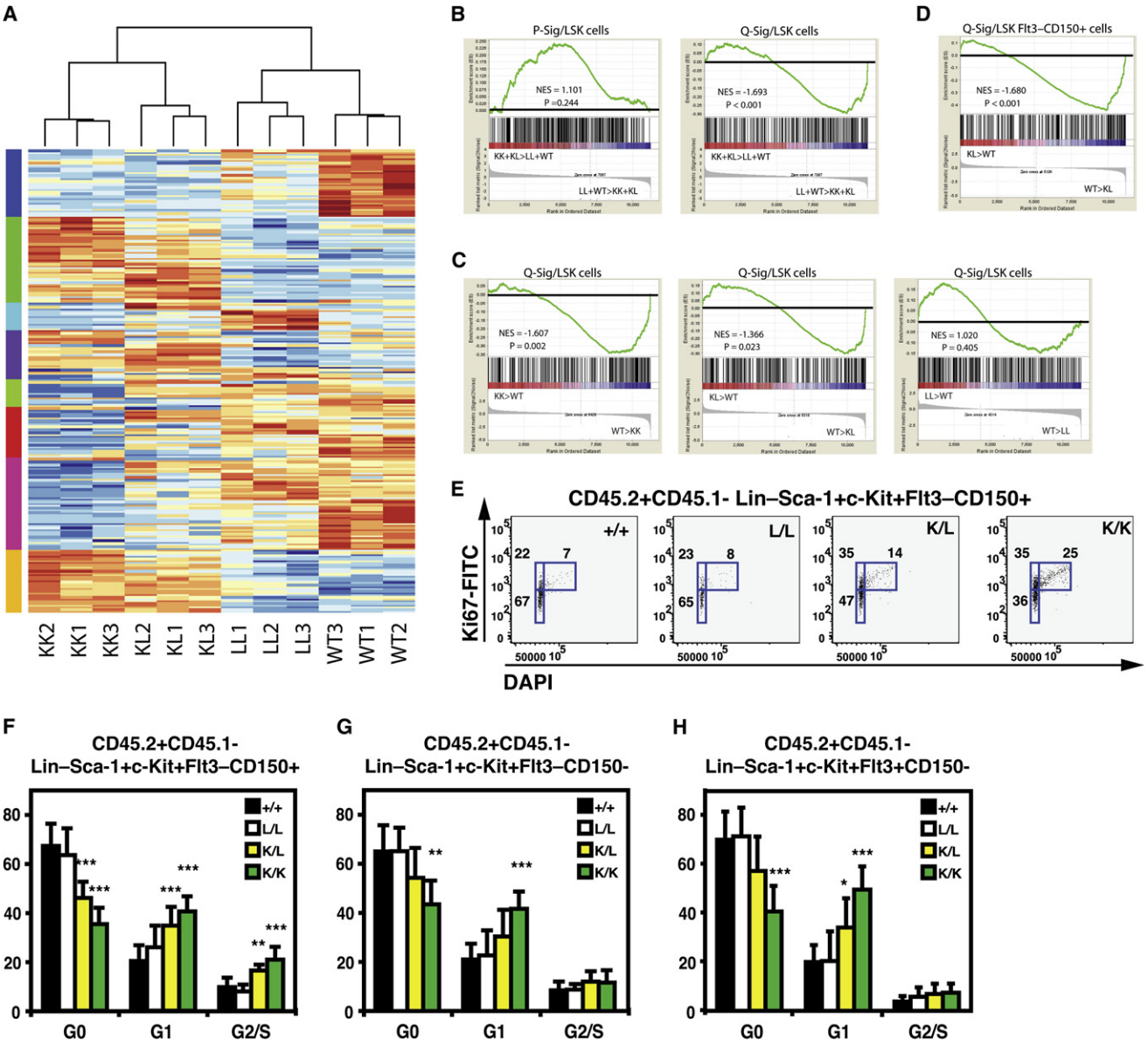

Figure 3. C terminal *Cebpa* Mutations Increase HSC Proliferation

(A) Unsupervised clustering of control and *Cebpa* mutant LSK populations using the union of differences between individual genotypes observed by LIMMA analysis of all pairwise combinations. The genes were K means clustered (n = 9) and clusters are color coded on the left side bar.

(B) GSEA comparison of the KK+KL genotypes against the LL+WT genotypes for enrichment/depletion of proliferation (proliferation associated gene expression; left panel) and quiescence (Q Sig; right panel) associated gene expression. The normalized enrichment scores (NES) and p values are indicated on each plot.

(C) Similar analysis as in (B) for Q Sig depletion in pairwise comparisons of WT and KK, WT and KL, and WT and LL (left to right) LSK populations.

(D) Depletion of Q Sig genes in K/L LT HSCs analyzed as in (B).

(E–H) Flow cytometric analysis of the cell cycle of FL derived LT HSC, ST HSC, and MPP. Representative contour plots in the top row show the gating strategy for the analysis (shown for the WT FL cells). Cell cycle phases were defined as G0 (Ki67$^-$, DAPI^{lo}), G1 (Ki67$^+$, DAPI^{lo}), and G2/S (Ki67$^+$, DAPI^{hi}) as shown in the right most dot plot. Representative dot plots for the cell cycle analysis of LT HSC in four indicated *Cebpa* genotypes are shown in the second row. Numbers close to each gate show the percentage of cells in a cell cycle phase. Average values (six or seven mice per genotype, two independent experiment) are shown in the graphs in (F) for LT HSC, (G) for ST HSC, and (H) for LMPPs (*$p < 0.05$; **$p < 0.005$; ***$p < 0.0005$, Student's t test). In all panels, error bars represent standard deviations.

knockin mutations specifically increased the proliferative capacity of committed myeloid progenitors, but not megakaryocyte-erythroid progenitors (Kirstetter et al., 2008; Porse et al., 2005). If this population were particularly susceptible to transformation, the ability to form committed myeloid cells would become rate limiting during tumor development. Because complete loss of C/EBPα was found to block myeloid lineage commitment at the CMP-GMP transition, it is possible that the

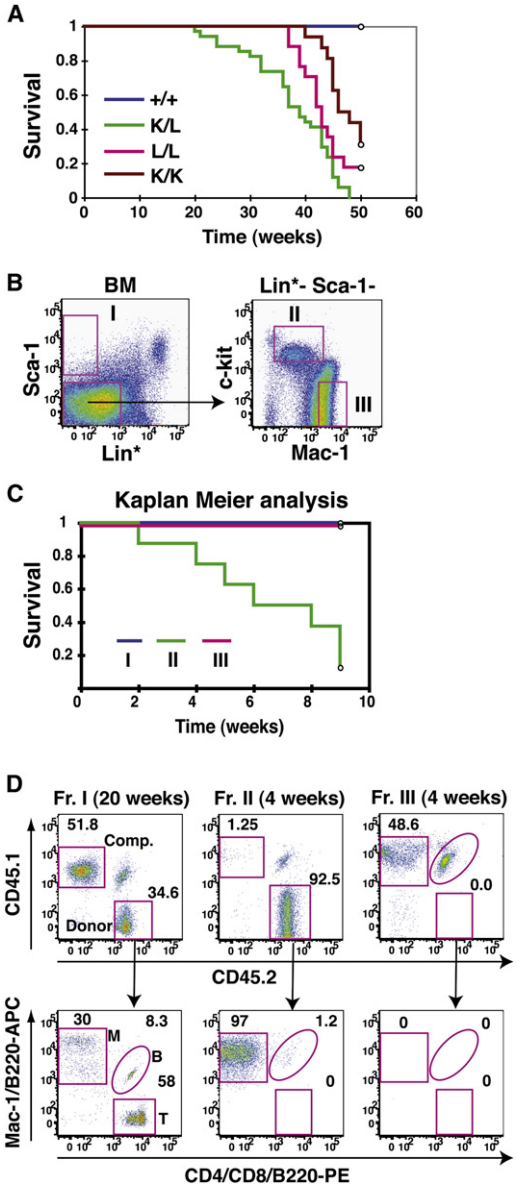

Figure 4. *Cebpa* Mutant Bone Marrow Chimeras Develop AML

(A) Kaplan Meier survival analysis of mice transplanted with +/+, L/L, K/L, and K/K FL cells showing the accelerated death in K/L transplanted animals, and a delay in tumor progression in K/K transplanted mice, each with respect to L/L transplanted mice. The number of animals from four independent experiments is included in the analysis, and the statistical significance (log rank analysis) for mice survival differences is shown to the right of the plot.

(B) Gating strategy for K/L tumor fractionation in tumor retransplantation experiments. Total BM cells were sorted as fractions I (Lin*$^-$Sca 1$^+$), II (Lin* $^{/lo}$ c Kit$^+$Mac 1 $^{/lo}$), and III (Lin* $^{/lo}$ c kit Mac 1+). The modified Lin* lineage cocktail excludes erythroid and lymphoid, but not myeloid, cells. Two thousand cells of each fraction were transplanted along with 2.5 × 105 helper bone marrow cells into the tail vein of lethally irradiated recipients, and animals were monitored for tumor development.

(C) Kaplan Meier survival curve for mice transplanted with cells of fractions I, II, and III showing lethality only in fraction II transplanted animals.

(D) Representative dot plots of PB analysis from K/L fraction I (left panels), fraction II (middle panels), and fraction III (right panel) transplanted animals at indicated time points, showing contribution of helper (CD45.1$^+$) and donor derived cells (CD45.2$^+$) (top row) and a distribution of myeloid (Mac 1$^+$), B (B220$^+$), and T cell lineages (CD4/CD8$^+$) within engrafted CD45.2$^+$ cells. Percentages indicate the proportion of gated populations within CD45.2$^+$ cells.

immature phenotype and relatively slow progression of K/K tumorigenesis was due to a block in formation of the committed myeloid progenitors. Using the classification of Akashi et al. (2000), we observed that GMP formation (defined as Lin$^-$Sca-1$^-$c-Kit$^+$IL-7rα$^-$CD34$^+$FcγII/III$^+$) was normal in L/L progenitors compared with +/+ controls, consistent with our previous results (Kirstetter et al., 2008). In contrast, GMP levels were lower in K/L progenitors and virtually absent in K/K progenitors, whereas the cotransplanted wild-type CD45.1 progenitors differentiated normally (Figure S2). Similar results were obtained with the more recent classification of Pronk et al. (2007). Here, GMPs are defined as Lin$^-$Sca-1$^-$c-Kit$^+$CD150$^-$FcγII/III$^+$ (Figure 6A). Importantly, the difference in GMP production between K/L and K/K progenitors was significant (Figure 6B), and only K/L progenitors gave rise to detectable myeloid-committed bone marrow (BM) cells (defined as Mac-1$^+$; Figure 6C), with both K/K and K/L cells generating similar number of bone marrow B cells. The lack of myeloid progression of K/K leukemias may therefore be explained by a severe and persistent block in the formation of committed myeloid progenitors, which is the cell population rendered susceptible to transformation by C/EBPα loss of function (Kirstetter et al., 2008; Porse et al., 2005). In the absence of committed progenitor transformation, a different, most likely erythroid, target cell is transformed, but with slower kinetics or less malignant phenotype, explaining the delay in K/K tumorigenesis relative to K/L tumors.

HSCs and multipotent progenitors have been observed to express at low levels genes characteristic of the lineages for which they have developmental potential, a phenomenon known as lineage priming (Hu et al., 1997; Mansson et al., 2007). Because it was recently found that separation of the myeloid lineages from the lymphoid and megakaryocytic/erythroid (Mk/E) lineages may occur already within the LSK compartment (Adolfsson et al., 2005; Pronk et al., 2007), we investigated whether the myeloid lineage commitment defect in K/K and K/L progenitors was evident at the HSC level. Using the previously defined Mk/E and myeloid-specific gene sets to analyze the LSK microarray data, we observed that myeloid genes were strongly depleted from K/K and K/L LSK cells (normalized enrichment scores [NES] < −2.5; p < 0.001), but less severely so in L/L LSK cells (NES = −1.432; p = 0.003) (Figure 6D), mirroring the subsequent lineage commitment defect. Conversely, MkE programming was significantly increased in K/K LSK cells, but not in K/L or L/L LSK cells (Figure S3). By dividing the MkE gene set into an E-specific and Mk-specific component, it was observed that the MkE enrichment in K/K LSK cells was due to increased erythroid gene expression (Figure 6E and Figure S3). We further investigated whether altered lineage programming was observed in the LT-HSC fraction: in K/L LT-HSCs, GM-specific genes were significantly depleted and E-specific genes were upregulated (Figures 6F and 6G). The more significant E-specific readout in the K/L LT-HSC fraction relative to total LSK cells was probably due to the generally high level of MkE priming in this cell population (Mansson et al., 2007). The relatively low level of *Cebpa* expression in the LT-HSC fraction

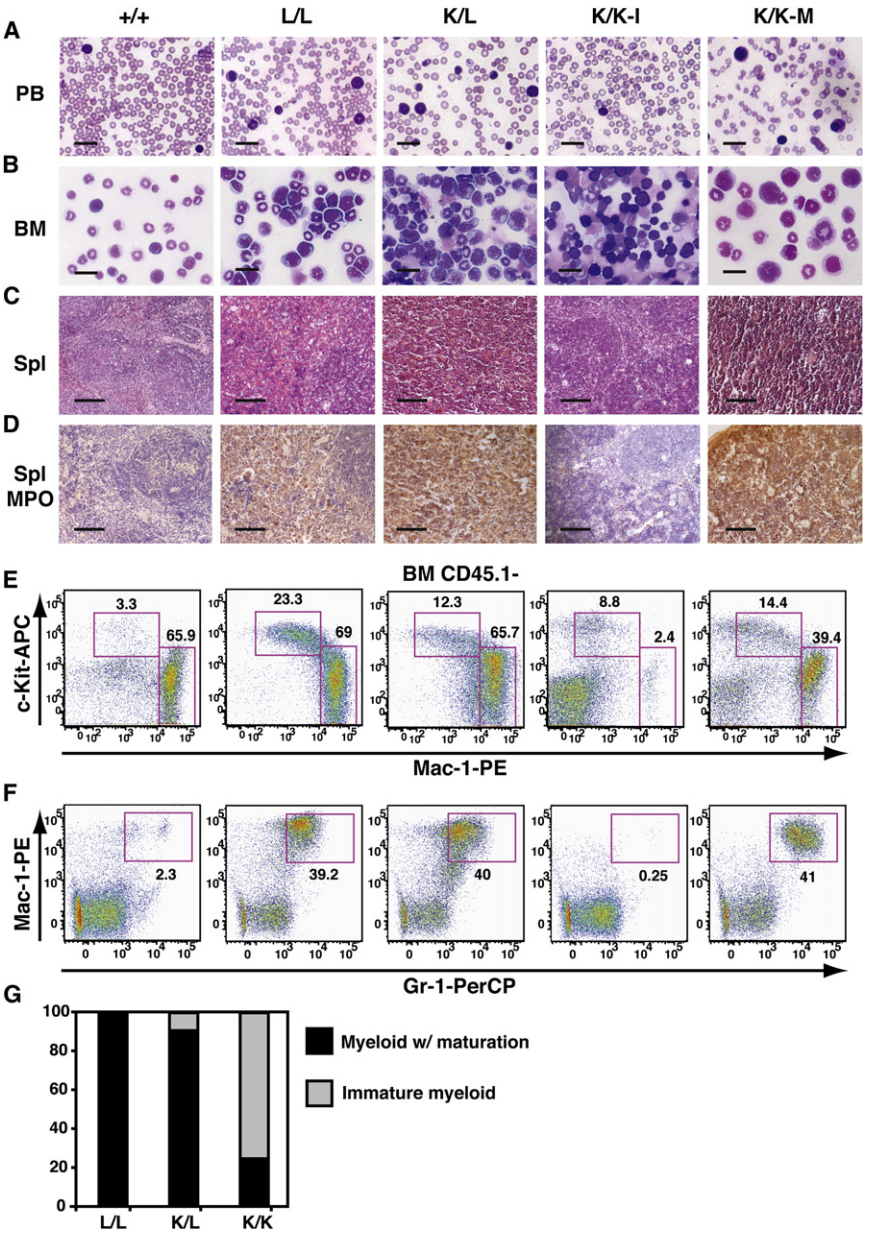

Figure 5. Different Myeloid Maturation of *Cebpa* Mutant AMLs

(A and B) Increased blast cells occurrence in PB (A) and BM (B) in leukemic mice as analyzed by May Grünwald/Gimsa staining of peripheral blood smears and BM cytospins. Scale bars represent 20 μm.

(C and D) Altered splenic architecture in L/L, K/L, and K/K M leukemic animals as analyzed by H&E staining of splenic sections (original magnifi cation, 10×) and infiltration of leukemic MPO^+ cells into spleen as seen in myeloperoxidase (MPO) staining of spleen tissue sections (D). Scale bars represent 1 mm.

(E) Representative FACS analysis of BM cells in control and leukemic mice at 8 months after trans plantation with FL cells of different *cebpa* genotypes (indicated in A). Donor cells ($CD45.1^-CD45.2^+$) were analyzed for the surface expression of c Kit and Mac 1. The percentages of each population relative to the total live BM cells are shown next to each gate.

(F) Flow cytometric analysis of splenocytes iso lated from control and leukemic mice revealed infiltration of myeloid Mac $1^+Gr\ 1^+$ cells into spleen. The frequency of gated population relative to total live splenocytes is shown next to the gate.

(G) Tumor phenotype distribution in mice trans planted with K/K (n = 12), K/L (n = 22), and L/L (n = 14) cells.

raised the issue of whether expression was restricted to a subpopulation of LT-HSCs. The altered lineage-specific gene expression pattern indicated that this could be addressed by measuring single-cell E-lineage priming in the LT-HSC population. If E-priming was expanded to the majority of cells, this would be consistent with *Cebpa* being expressed throughout the compartment. We tested this using KK LT-HSCs (the genotype where the effect of lineage priming was stronger), and found that the number of *Gata1*, *Epor,* and *Klf1* expressing cells was strongly increased relative to wild-type control cells, whereas expression of *Csf3r* (which is a C/EBPα target gene encoding the G-CSF-R) was decreased (Figure S4). In particular *Gata1* expression was observed in virtually all KK LT-HSCs. This indicated that the effect of *Cebpa* mutation was fairly uniform across the LT-HSC compartment and showed that the loss of C/EBPα function led to altered lineage priming also at the single-cell level.

DISCUSSION

The results presented here provide direct genetic evidence that leukemogenic *Cebpa* mutations induce the loss of quiescence in, and consequently expansion of, premalignant HSCs/MPPs in a cell-intrinsic manner. In addition, we show that the presence of C-terminal *Cebpa* mutations skews the lineage programming of HSCs, decreasing myeloid gene expression and increasing erythroid-specific gene expression, concomitant with a subsequent myeloid differentiation defect, providing a direct link between expression of lineage-specific programs in HSCs and their lineage potential. Finally, we find that the most efficient leukemogenesis occurs when premalignant HSC expansion (induced by C-terminal *Cebpa* mutation) is combined with residual myeloid lineage commitment (maintained by the N-terminal *Cebpa* mutation), providing a model for *CEBPA* mutant leukemia development that explains the prevalence of tumors carrying one of each of the two mutation types.

Modeling of human leukemogenesis in the mouse has relied to a large extent on the use of retroviral transduction to introduce oncogenes into the stem cell/progenitor compartment. Although this is a powerful system for the verification of leukemogenic potential and analysis of oncogene synergy, it has limitations

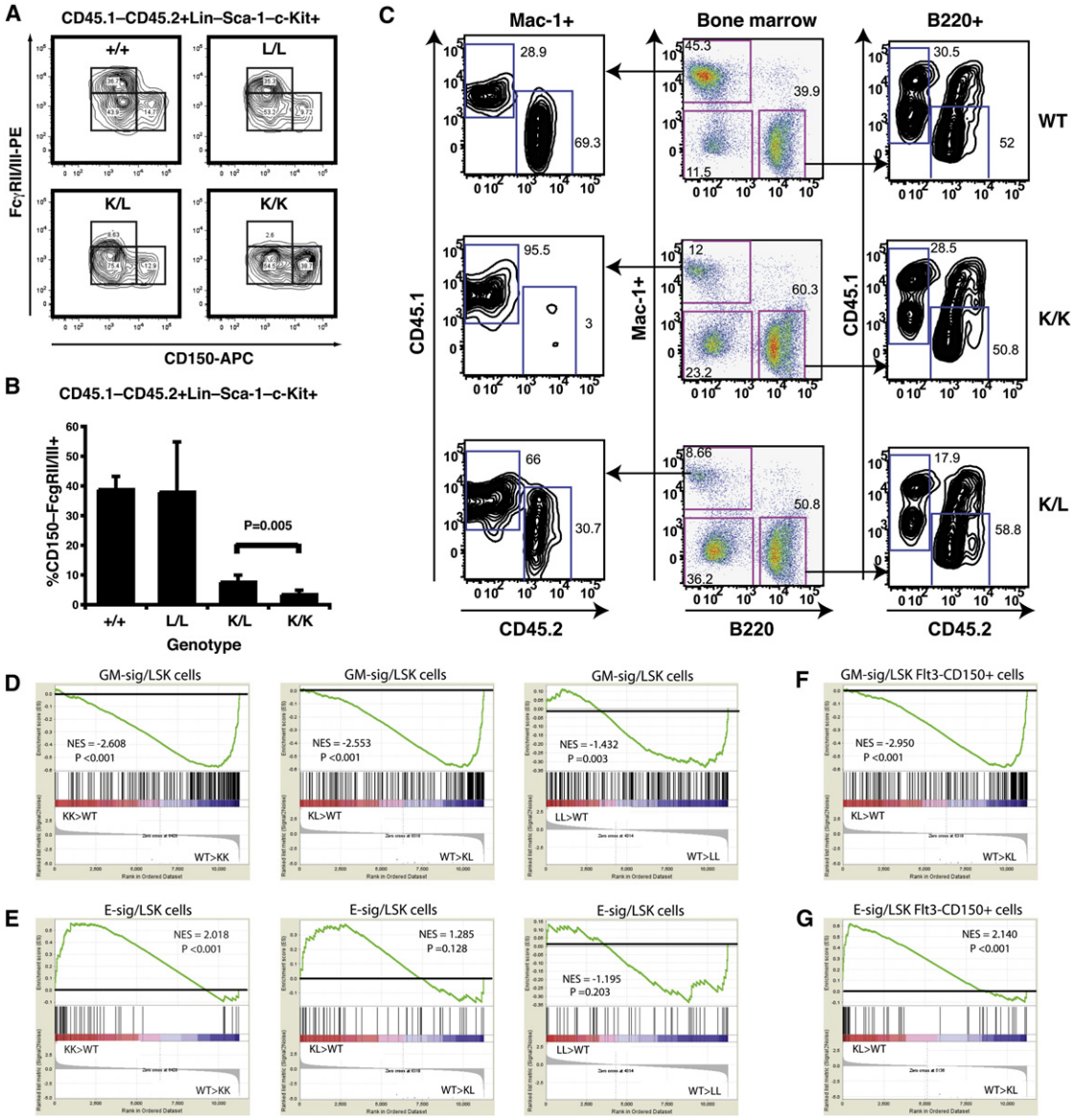

Figure 6. Leukemogenic *Cebpa* Mutations Control HSC Myeloid Gene Expression and Committed Myeloid Progenitor Formation

(A) Flow cytometric analysis of myeloid differentiation potential of FL derived cells of different genotypes at 4.5 weeks after transplantation. Lineage/Sca 1/IL7Rα$^-$ cells were gated and analyzed for the surface expression of c Kit, CD150, and FcγRII/III for separation of GMPs (c Kit$^+$CD150$^-$FcγRII/III+) from pre GM (c Kit$^+$CD150$^-$FcγRII/III$^-$) progenitors. Representative contour plots for each genotype are shown.

(B) Average values for five or more animals per genotype analyzed as in (A) are shown in graph. Error bars indicate standard deviations.

(C) BM cells from transplanted animals were stained for CD45.1, CD45.2, Mac 1, and B220 expression. The distribution of allotypes was analyzed for the B220$^+$ (right panels) and Mac 1$^+$ (left panels) experimental population. Numbers indicate the percentage of the gated populations.

(D and E) GSEA analysis of myeloid (upper panels) and (E) erythroid (lower panels) gene expression in *Cebpa* mutant LSK populations. Each population was compared individually with WT control profiles. The NES and p values are indicated on each plot.

(F and G) Similar analysis as in (D) and (E) for K/L LT HSCs.

when it comes to studying stem cell populations due to the heterogeneity of transduced populations and nonphysiological levels of expression. The use of knockin mutagenesis has been employed to study the MLL-AF9, RUNX1-ETO, CBFβ-SMMHC, and FLT3-ITD mutations (Chen et al., 2008; Higuchi et al., 2002; Kuo et al., 2006; Lee et al., 2007) in addition to C/EBPα (Kirstetter et al., 2008). Only in the case of CBFβ-SMMHC was the effect of the mutation of HSC function evaluated, and repopulating activity observed to be decreased (Kuo et al., 2006). The effect of Runx1-Eto on HSC function was not analyzed (Higuchi et al., 2002); however, using the same genetic model, we have observed no expansion or competitive advantage of HSCs expressing this oncogene (E.M. and C.N., unpublished data). The Flt3-ITD mutation did in its homozygous state lead

to a mild expansion of LSK cells, but no leukemia developed in this case (Lee et al., 2007). Both LSK expansion and leukemia was observed in the case of Mll-Af9, but in a noncompetitive setting (Chen et al., 2008). The present study may therefore provide an example of a leukemogenic mutation that confers a selective advantage to mutant HSCs in a competitive situation. At the cellular level, HSCs carrying *Cebpa* K/K and K/L genotypes were found to evade the normal homeostatic control of HSC numbers: the mutant population expanded in an otherwise wild-type bone marrow environment, demonstrating that expansion is a cell intrinsic property conferred by the *Cebpa* mutation. This expansion was associated with decreased quiescence of the LSK population. Importantly, the LT-HSC enriched LSKCD150^{+}Flt3^{-} subset showed increased cycling in the K/K and K/L *Cebpa* genotypes. The expansive phenotype was associated with downregulation of gene expression normally associated with the quiescent state (Venezia et al., 2004). These results identify C/EBPα as a cell-intrinsic negative regulator of HSC cell-cycle progression and homeostasis, and indicate that C/EBPα regulates a quiescence-associated gene expression program. It is clear, however, that expansion of FL HSC is not affected by *Cebpa* mutations because similar numbers of HSCs were present in FL from the various *Cebpa* genotypes. The proliferation of FL HSCs is very rapid with a cycling time of ca. 11 hr (Nygren et al., 2006), as opposed to the highly quiescent HSC in the BM. Given that *Cebpa* mutation seems to affect principally quiescence-associated gene expression, the lack of quiescence of FL-HSCs could therefore explain the absence of *Cebpa* mutant FL expansion.

In addition, our results provide additional insights into the role of lineage commitment in myeloid leukemogenesis. It has been assumed that AML LICs were phenotypically similar to HSCs (Bonnet and Dick, 1997; Lapidot et al., 1994), and that the unilineage property of most AMLs was due to lineage bias during LIC differentiation. However, recent results indicate that LICs in human AML may include committed progenitors in many cases (Taussig et al., 2008), a fact previously obscured by their selective elimination by the residual immune system of the NOD/SCID host when conjugated with the anti-CD38 antibody used to discriminate progenitors from stem cells. The results obtained here as well as in earlier studies of myeloid leukemias arising in *Cebpa* mutant knockin mice (Kirstetter et al., 2008), or after viral transduction of MOZ-TIF2 (Huntly et al., 2004) or MLL fusion proteins (Cozzio et al., 2003; Somervaille and Cleary, 2006), all support the ability of committed progenitors to sustain AML. In these leukemias, the mutation directly affects myeloid progenitors by increasing their proliferative capacity (but not that of, for example, megakaryocyte-erythroid progenitors [Huntly et al., 2004; Kirstetter et al., 2008]), indicating that lineage selection occurs through the specific effect of these mutations on the myeloid progenitors, leading to preferential generation of a myeloid unilineage LIC. This view is further supported by our recent finding that *Cebpa* mutations introduce a myeloid lineage bias in leukemias arising after retroviral insertion mutagenesis (Hasemann et al., 2008). This model does not require that the mutations instruct HSCs to undergo myeloid lineage commitment. In fact, the most highly leukemogenic combination of *Cebpa* mutations (K/L genotype) impairs myeloid lineage commitment. As previously demonstrated, homozygosity (but not heterozygosity) for leukemogenic *Cebpa* mutations selectively confers a proliferative phenotype on committed myeloid progenitors (Kirstetter et al., 2008), consistent with the idea that the selective ability of these mutations to render committed myeloid progenitors susceptible to transformation, and not their lineage instructive properties, enables them to preferentially cause unilineage myeloid leukemia.

Finally, our results demonstrate that C/EBPα can act at the LT-HSC stage to regulate lineage-specific gene expression in a global manner: loss of C/EBPα DNA binding activity led to a coordinated downregulation of myeloid-specific gene expression (in the K/L and K/K LSK cells) and upregulation of erythroid-specific genes (K/K LSK cells and K/L LT-HSCs). The disruption of HSC lineage programming precedes and parallels the subsequent defect in myeloid lineage commitment, providing evidence that HSC lineage priming is a direct determinant of downstream lineage potential. In this model, the more severe lineage commitment defect of the K/K HSCs may be explained by the combined downregulation of the myeloid and upregulation of the erythroid program, leading to a virtually complete bias away from myeloid progenitor formation. It is interesting to note that comparison between *CEBPA* mutant and nonmutant AML revealed that several erythroid-specific genes, including *GATA1* and *EPOR*, were enriched in the *CEBPA* mutant cases (Marcucci et al., 2008). Although caution needs to be applied in comparison to the present data because the cell populations sampled are very different (purified stem cells versus bulk tumor), this indicates that *CEBPA* mutation leads to derepression of erythroid gene expression in human AML, and possibly also erythroid bias of progenitor formation. This issue, however, clearly needs further investigation.

In conclusion, we find that the clinical pattern of *CEBPA* mutations can be explained by the ability of biallelic N- and C-terminal mutations to expand premalignant stem cells, combined with the residual capacity to commit to the myeloid lineage. At a more general level, these results demonstrate that the actions of leukemogenic mutations are not confined to the final transformed cell population: the processes that select the clinical *CEBPA* mutation pattern (HSC expansion, lineage commitment) affect cells located upstream of the final transformed progenitor in the hematopoietic hierarchy. Thus, critical functions of oncogenic mutations may be executed prior to actual cellular transformation, and in cells that reside upstream of the final transformed cell in the differentiation hierarchy.

EXPERIMENTAL PROCEDURES

Mouse Strains

The *Cebpa* Lp30 allele has been described previously. The K313KK mutation was generated by inserting an additional lysine into position 314 in the C/EBPα coding sequence, with the targeting strategy previously described (Porse et al., 2001). Mouse lines were maintained on a mixed C57Bl/6 129/Ola background (ca. 75% C57Bl/6 and 25% 129/Ola) under SPF conditions, according to EMBL institutional and Italian National guidelines. All procedures were approved by the EMBL Monterotondo Ethical Committee.

Bone Marrow Transplantation

E14.5 FL were obtained from intercrosses of *Cebpa*$^{L/+}$ and *Cebpa*$^{K/+}$ mice, as appropriate. FL cell suspensions were prepared by mechanically disrupting FLs passing through the 18 G needle in HBSS 2% fetal calf serum (FCS) and cryopreserved in freezing media composed of 70% FCS, 10% dimethyl sulf oxide, and 20% IMDM). CD45.1/2 recipients were generated by intercrossing

C57Bl/6 CD45.1 (Harlan) and C57Bl/6 CD45.2 (EMMA, Monterotondo, Italy) mice, and lethally irradiated as described (Kirstetter et al., 2008). 125,000 FL cells (CD45.2) were cotransplanted with 500,000 competitor BM cells (CD45.1). For transplantation of leukemic cells, 1 5.000 sorted leukemia cells (CD45.2) were cotransplanted with 250,000 1,000,000 competitor cells (CD45.1).

Flow Cytometry and Cell Sorting

Cell sorting and flow cytometric analysis were performed essentially as described elsewhere (Kirstetter et al., 2008). Details of staining protocols and antibody dilutions can be found in Supplemental Experimental Procedures.

Real-Time PCR Analysis

For measurement of mRNA quantitative real time polymerase chain reaction (RT PCR), total RNA was isolated with an RNeasy mini kit (QIAGEN) from puri fied hematopoietic stem cell fractions, digested with DNase I for removal of genomic DNA contamination, and used for reverse transcription with oligo(dT) primer according to the manufacturer's instructions (T primed First Strand Kit, Amersham Biosciences). Triplicate RT PCR reactions were performed with 100 cell equivalents of RNA and normalized to *Hprt1* (hypoxanthine guanine phosphoribosyl transferase 1) with TaqMan probes and TaqMan universal PCR master mix according to the manufacturer's instructions (Applied Biosys tems, Hammonton, NJ). Fold expression relative to *Hprt1* was calculated with the comparative Ct (2^{-dCt}) method.

Histology

Sections of spleen, liver, lung, or kidney were prepared as described elsewhere (Porse et al., 2001) and stained with hematoxylin eosin (H&E) or used for immu nohistochemistry with rabbit anti MPO (A0398; DAKO) as primary antibody. Binding of primary antibodies was detected with an Envision+ HRP (DAB) detection kit (DAKO), in accordance with the manufacturer's recommenda tions. After that, the sections were counterstained with hematoxylin.

Microarray Analysis

Total RNA from sorted CD45.1$^-$CD45.2$^+$Lin Sca 1$^+$c Kit$^+$ (LSK) cells from CD45.1/2 mice competitively transplanted with CD45.2 experimental and CD45.1 competitor bone marrow (2 5000 cells/sample) was hybridized to Affy metrix MOE430 2.0 microarrays after two rounds of linear amplification by the SCIBLU genomics facility (University of Lund, Sweden) and analyzed as described previously (Kirstetter et al., 2008), except that data were clustered by K means. Normalized data were filtered for minimal expression and then tested for gene set enrichment using GSEA v2.0 (Subramanian et al., 2005) (http://www.broad.mit.edu/gsea/). Each genotype (KK, KL, and LL for LSK; KL for LT HSC) was compared with the control in a separate test. Gene sets were curated from Venezia et al. (2004) and Mansson et al. (2007). The Mk and E specific gene sets were generated from the MkE gene set (Mansson et al., 2007) by selecting genes showing a >1.5 fold overexpression in Mk versus E and E versus Mk differentiated cells, respectively. GSEA enrichment results were filtered for statistical significance using a nominal p value threshold of 0.05.

Lineage Priming

Single cell lineage priming analysis was carried out as previously described (Adolfsson et al., 2005; Mansson et al., 2007).

Statistical Analysis

Statistical significance was determined with Student's t test, except for Ka plan Meier survival comparisons, where the log rank test was used (calculated with XLStat software; Addinsoft, Paris, France).

ACCESSION NUMBERS

Microarray data have been deposited in the ArrayExpress database under the accession numbers E TABM 694 and E TABM 695.

SUPPLEMENTAL DATA

Supplemental Data include Supplemental Experimental Procedures, four figures, and two tables and can be found with this article online at http://www.cell.com/cancer cell/supplemental/S1535 6108(09)00344 4.

ACKNOWLEDGMENTS

The authors thank the EMBL FACS facility for expert cell sorting assistance and the SCIBLU genomics facility, University of Lund, for microarray analysis. This work was funded by the European Commission (EuroCSC STREP), the Associazione Italiana per la Ricerca sul Cancro (AIRC), and the Swedish Research Council (HematoLinne grant). O.B. was a recipient of an HFSP post doctoral fellowship. S.E.J. is the recipient of an MRC strategic appointment award.

Received: April 16, 2009
Revised: September 29, 2009
Accepted: September 29, 2009
Published: November 2, 2009

REFERENCES

Adolfsson, J., Mansson, R., Buza Vidas, N., Hultquist, A., Liuba, K., Jensen, C.T., Bryder, D., Yang, L., Borge, O.J., Thoren, L.A., et al. (2005). Identification of Flt3+ lympho myeloid stem cells lacking erythro megakaryocytic potential a revised road map for adult blood lineage commitment. Cell *121*, 295 306.

Akashi, K., Traver, D., Miyamoto, T., and Weissman, I.L. (2000). A clonogenic common myeloid progenitor that gives rise to all myeloid lineages. Nature *404*, 193 197.

Bonnet, D., and Dick, J.E. (1997). Human acute myeloid leukemia is organized as a hierarchy that originates from a primitive hematopoietic cell. Nat. Med. *3*, 730 737.

Chen, W., Kumar, A.R., Hudson, W.A., Li, Q., Wu, B., Staggs, R.A., Lund, E.A., Sam, T.N., and Kersey, J.H. (2008). Malignant transformation initiated by Mll AF9: Gene dosage and critical target cells. Cancer Cell *13*, 432 440.

Cozzio, A., Passegue, E., Ayton, P.M., Karsunky, H., Cleary, M.L., and Weiss man, I.L. (2003). Similar MLL associated leukemias arising from self renewing stem cells and short lived myeloid progenitors. Genes Dev. *17*, 3029 3035.

Hasemann, M.S., Damgaard, I., Schuster, M.B., Theilgaard Monch, K., Soren sen, A.B., Mrsic, A., Krugers, T., Ylstra, B., Pedersen, F.S., Nerlov, C., and Porse, B.T. (2008). Mutation of C/EBPalpha predisposes to the development of myeloid leukemia in a retroviral insertional mutagenesis screen. Blood *111*, 4309 4321.

Heath, V., Suh, H.C., Holman, M., Renn, K., Gooya, J.M., Parkin, S., Klarmann, K.D., Ortiz, M., Johnson, P., and Keller, J. (2004). C/EBPalpha deficiency results in hyperproliferation of hematopoietic progenitor cells and disrupts macrophage development in vitro and in vivo. Blood *104*, 1639 1647.

Higuchi, M., O'Brien, D., Kumaravelu, P., Lenny, N., Yeoh, E.J., and Downing, J.R. (2002). Expression of a conditional AML1 ETO oncogene bypasses embryonic lethality and establishes a murine model of human t(8;21) acute myeloid leukemia. Cancer Cell *1*, 63 74.

Hu, M., Krause, D., Greaves, M., Sharkis, S., Dexter, M., Heyworth, C., and Enver, T. (1997). Multilineage gene expression precedes commitment in the hemopoietic system. Genes Dev. *11*, 774 785.

Huntly, B.J., Shigematsu, H., Deguchi, K., Lee, B.H., Mizuno, S., Duclos, N., Rowan, R., Amaral, S., Curley, D., Williams, I.R., et al. (2004). MOZ TIF2, but not BCR ABL, confers properties of leukemic stem cells to committed murine hematopoietic progenitors. Cancer Cell *6*, 587 596.

Jordan, C.T., Astle, C.M., Zawadzki, J., Mackarehtschian, K., Lemischka, I.R., and Harrison, D.E. (1995). Long term repopulating abilities of enriched fetal liver stem cells measured by competitive repopulation. Exp. Hematol. *23*, 1011 1015.

Kelly, L.M., and Gilliland, D.G. (2002). Genetics of myeloid leukemias. Annu. Rev. Genomics Hum. Genet. *3*, 179 198.

Kirstetter, P., Schuster, M.B., Bereshchenko, O., Moore, S., Dvinge, H., Kurz, E., Theilgaard Monch, K., Mansson, R., Pedersen, T.A., Pabst, T., et al. (2008). Modeling of C/EBPalpha mutant acute myeloid leukemia reveals a common expression signature of committed myeloid leukemia initiating cells. Cancer Cell *13*, 299 310.

Kottaridis, P.D., Gale, R.E., Langabeer, S.E., Frew, M.E., Bowen, D.T., and Linch, D.C. (2002). Studies of FLT3 mutations in paired presentation and relapse samples from patients with acute myeloid leukemia: Implications for the role of FLT3 mutations in leukemogenesis, minimal residual disease detection, and possible therapy with FLT3 inhibitors. Blood *100*, 2393–2398.

Kuo, Y.H., Landrette, S.F., Heilman, S.A., Perrat, P.N., Garrett, L., Liu, P.P., Le Beau, M.M., Kogan, S.C., and Castilla, L.H. (2006). Cbf beta-SMMHC induces distinct abnormal myeloid progenitors able to develop acute myeloid leukemia. Cancer Cell *9*, 57–68.

Lapidot, T., Sirard, C., Vormoor, J., Murdoch, B., Hoang, T., Caceres-Cortes, J., Minden, M., Paterson, B., Caligiuri, M.A., and Dick, J.E. (1994). A cell initiating human acute myeloid leukaemia after transplantation into SCID mice. Nature *367*, 645–648.

Lee, B.H., Tothova, Z., Levine, R.L., Anderson, K., Buza-Vidas, N., Cullen, D.E., McDowell, E.P., Adelsperger, J., Frohling, S., Huntly, B.J., et al. (2007). FLT3 mutations confer enhanced proliferation and survival properties to multipotent progenitors in a murine model of chronic myelomonocytic leukemia. Cancer Cell *12*, 367–380.

Leroy, H., Roumier, C., Huyghe, P., Biggio, V., Fenaux, P., and Preudhomme, C. (2005). CEBPA point mutations in hematological malignancies. Leukemia *19*, 329–334.

Mansson, R., Hultquist, A., Luc, S., Yang, L., Anderson, K., Kharazi, S., Al-Hashmi, S., Liuba, K., Thoren, L., Adolfsson, J., et al. (2007). Molecular evidence for hierarchical transcriptional lineage priming in fetal and adult stem cells and multipotent progenitors. Immunity *26*, 407–419.

Marcucci, G., Maharry, K., Radmacher, M.D., Mrozek, K., Vukosavljevic, T., Paschka, P., Whitman, S.P., Langer, C., Baldus, C.D., Liu, C.G., et al. (2008). Prognostic significance of, and gene and microRNA expression signatures associated with, CEBPA mutations in cytogenetically normal acute myeloid leukemia with high-risk molecular features: A Cancer and Leukemia Group B Study. J. Clin. Oncol. *26*, 5078–5087.

Moore, M.A. (2005). Converging pathways in leukemogenesis and stem cell self-renewal. Exp. Hematol. *33*, 719–737.

Nerlov, C. (2004). C/EBPalpha mutations in acute myeloid leukaemias. Nat. Rev. Cancer *4*, 394–400.

Nerlov, C. (2007). The C/EBP family of transcription factors: A paradigm for interaction between gene expression and proliferation control. Trends Cell Biol. *17*, 318–324.

Nygren, J.M., Bryder, D., and Jacobsen, S.E. (2006). Prolonged cell cycle transit is a defining and developmentally conserved hemopoietic stem cell property. J. Immunol. *177*, 201–208.

Pabst, T., and Mueller, B.U. (2007). Transcriptional dysregulation during myeloid transformation in AML. Oncogene *26*, 6829–6837.

Porse, B.T., Bryder, D., Theilgaard-Monch, K., Hasemann, M.S., Anderson, K., Damgaard, I., Jacobsen, S.E., and Nerlov, C. (2005). Loss of C/EBP alpha cell cycle control increases myeloid progenitor proliferation and transforms the neutrophil granulocyte lineage. J. Exp. Med. *202*, 85–96.

Porse, B.T., Pedersen, T.A., Xu, X., Lindberg, B., Wewer, U.M., Friis-Hansen, L., and Nerlov, C. (2001). E2F repression by C/EBPalpha is required for adipogenesis and granulopoiesis in vivo. Cell *107*, 247–258.

Pronk, C.J., Rossi, D.J., Mansson, R., Attema, J.L., Norddahl, G.L., Chan, C.K., Sigvardsson, M., Weissman, I.L., and Bryder, D. (2007). Elucidation of the phenotypic, functional, and molecular topography of a myeloerythroid progenitor cell hierarchy. Cell Stem Cell *1*, 428–442.

Shih, L.Y., Huang, C.F., Wu, J.H., Lin, T.L., Dunn, P., Wang, P.N., Kuo, M.C., Lai, C.L., and Hsu, H.C. (2002). Internal tandem duplication of FLT3 in relapsed acute myeloid leukemia: A comparative analysis of bone marrow samples from 108 adult patients at diagnosis and relapse. Blood *100*, 2387–2392.

Shih, L.Y., Huang, C.F., Wu, J.H., Wang, P.N., Lin, T.L., Dunn, P., Chou, M.C., Kuo, M.C., and Tang, C.C. (2004). Heterogeneous patterns of FLT3 Asp(835) mutations in relapsed de novo acute myeloid leukemia: A comparative analysis of 120 paired diagnostic and relapse bone marrow samples. Clin. Cancer Res. *10*, 1326–1332.

Shih, L.Y., Liang, D.C., Huang, C.F., Wu, J.H., Lin, T.L., Wang, P.N., Dunn, P., Kuo, M.C., and Tang, T.C. (2006). AML patients with CEBPalpha mutations mostly retain identical mutant patterns but frequently change in allelic distribution at relapse: A comparative analysis on paired diagnosis and relapse samples. Leukemia *20*, 604–609.

Somervaille, T.C., and Cleary, M.L. (2006). Identification and characterization of leukemia stem cells in murine MLL-AF9 acute myeloid leukemia. Cancer Cell *10*, 257–268.

Subramanian, A., Tamayo, P., Mootha, V.K., Mukherjee, S., Ebert, B.L., Gillette, M.A., Paulovich, A., Pomeroy, S.L., Golub, T.R., Lander, E.S., and Mesirov, J.P. (2005). Gene set enrichment analysis: A knowledge-based approach for interpreting genome-wide expression profiles. Proc. Natl. Acad. Sci. USA *102*, 15545–15550.

Taussig, D.C., Miraki-Moud, F., Anjos-Afonso, F., Pearce, D.J., Allen, K., Ridler, C., Lillington, D., Oakervee, H., Cavenagh, J., Agrawal, S.G., et al. (2008). Anti-CD38 antibody-mediated clearance of human repopulating cells masks the heterogeneity of leukemia-initiating cells. Blood *112*, 568–575.

Venezia, T.A., Merchant, A.A., Ramos, C.A., Whitehouse, N.L., Young, A.S., Shaw, C.A., and Goodell, M.A. (2004). Molecular signatures of proliferation and quiescence in hematopoietic stem cells. PLoS Biol. *2*, e301.

Zhang, P., Iwasaki-Arai, J., Iwasaki, H., Fenyus, M.L., Dayaram, T., Owens, B.M., Shigematsu, H., Levantini, E., Huettner, C.S., Lekstrom-Himes, J.A., et al. (2004). Enhancement of hematopoietic stem cell repopulating capacity and self-renewal in the absence of the transcription factor C/EBP alpha. Immunity *21*, 853–863.